Remote Sensing Applications: Society and Environment 26 (2022) 100716

Contents lists available at ScienceDirect

Remote Sensing Applications: Society and Environment

journal homepage: www.elsevier.com/locate/rsase

Estimating $PM_{2.5}$ surface concentrations from AOD: A combination of SLSTR and MODIS

Jana Handschuh [a,*], Thilo Erbertseder [a], Martijn Schaap [b,c], Frank Baier [a]

[a] German Aerospace Center (DLR), Earth Observation Center, German Remote Sensing Data Center, Weßling, Germany
[b] Free University of Berlin (FUB), Institute of Meteorology, Berlin, Germany
[c] Netherlands Organization for Applied Scientific Research (TNO), Department of Climate, Air and Sustainability, Utrecht, the Netherlands

ARTICLE INFO

Keywords:
Aerosol optical depth (AOD)
Fine particulate matter ($PM_{2.5}$)
MODIS
SLSTR
Germany

ABSTRACT

Compared to surface in-situ observations, satellite data on aerosol optical depth (AOD) enables area-wide monitoring of tropospheric aerosols. However, coverage and reliability of satellite data products depend on atmospheric conditions and surface concentrations have to be retrieved from AOD. This study investigates the potential to produce reliable maps of $PM_{2.5}$ surface concentrations for Germany and parts of the surrounding countries using AOD based on observations by three different satellite sensors. For the first time, AOD retrievals from the Sea and Land Surface Temperature Radiometer (SLSTR) onboard Sentinel-3A are used together with those from the Moderate Resolution Imaging Spectroradiometer (MODIS) onboard the two NASA platforms Terra and Aqua. We investigate the differences and similarities of the three different satellite products in terms of coverage, resolution and algorithmic performances. Based on this analysis we examine the suitability and advantage of a combination of these data sets. We can substantiate an increase in mean daily coverage from a maximum of 10.2% for the individual products to 16.7% for the ensemble product. Using a semi-empirical linear regression model, we derive surface-level $PM_{2.5}$ concentrations and attain an overall correlation of 0.76 between satellite-derived and in-situ measured $PM_{2.5}$ concentrations. By considering surface measurements, the systematic error (bias) and the root mean square error (RMSE) can be significantly reduced. The general model performance is evaluated by a 5-fold cross validation and the relative prediction error (RPE).

1. Introduction

Due to its adverse effects on human health, ambient air pollution, including pollutants such as particulate matter, ozone, nitrogen dioxide and sulfur dioxide, has become an important field in modern research. Especially in urbanized and industrialized regions people are exposed to increased concentrations of harmful substances (European Environment Agency, 2021; World Health Organization, 2021). Fine particulate matter with aerodynamic diameters less than 2.5 μm ($PM_{2.5}$) was found to be the main pollutant causing serious health risks such as respiratory and cardiovascular diseases and even lung cancer (Beelen et al., 2014; Khomenko et al., 2021; Kloog et al., 2013; Lelieveld et al., 2020).

A better understanding of the spatial and temporal distribution of near surface $PM_{2.5}$ pollution is essential to assess the impact on the environment and to estimate potential health risks for the general public and vulnerable groups in particular (Sorek-Hamer et al., 2016). Therefore, an accurate comprehensive monitoring and mapping of ambient $PM_{2.5}$ concentrations is necessary.

* Corresponding author. German Aerospace Center (DLR), German Remote Sensing Data Center, Münchener Straße 20, 82234 Weßling, Germany.
E-mail address: jana.handschuh@dlr.de (J. Handschuh).

https://doi.org/10.1016/j.rsase.2022.100716
Received 17 August 2021; Received in revised form 3 February 2022; Accepted 21 February 2022
Available online 24 February 2022

Ground-based in-situ stations provide accurate and frequent measurements of $PM_{2.5}$ concentrations, but only for selected locations. Even with a well-developed station network, the density of measurements is insufficient to attain area-wide coverage of the aerosol distribution with its sources and sinks. In order to fill the information gaps between the stations, satellite observations have proven to be a valuable complement (Hoff and Christopher, 2009; Van de Kassteele et al., 2006). The aerosol load of the atmosphere is quantified by satellite retrievals of the aerosol optical depth (AOD), which describes the extinction of light by aerosol particles when passing through the atmosphere.

Multiple studies were performed to derive ground-level $PM_{2.5}$ concentrations from columnar AOD measurements for different regions worldwide. Most of them focus on the USA and China, only few were performed for Europe, including the Netherlands (Schaap et al., 2009), France (Kacenelenbogen et al., 2006), Italy (Di Nicolantonio et al., 2009, 2011) and the UK (Beloconi et al., 2016). Chu et al. (2016) published an overview on the different studies, listing the study regions, the used satellite products and the applied methods. A recent review article was published by Zhang et al. (2021), including latest methodological developments for $PM_{2.5}$ derivation from AOD. The most commonly used methods to derive $PM_{2.5}$ are observation-based approaches such as simple linear correlation (Engel-Cox et al., 2004; Koelemeijer et al., 2006; Toth et al., 2014), multiple linear regression (Kumar et al., 2013; Lai et al., 2014; Schaap et al., 2009; Zhang and Li, 2015), mixed-effect modelling (Chudnovsky et al., 2013; Kloog et al., 2015; Liu et al., 2007; Shi et al., 2016; Xie et al., 2015; You et al., 2015), geographically and temporally weighted regression (He and Huang, 2018; Hu et al., 2013; Song et al., 2014; Zou et al., 2016), land use regression (Li et al., 2018), Bayesian geostatistical modelling (Beloconi et al., 2018) and timely structure adaptive modelling (Fang et al., 2016). In recent years, also machine learning approaches have been developed. Chen et al. (2018), for example, used a random forest model to predict historical $PM_{2.5}$ concentrations in China and Just et al. (2020) applied an extreme gradient boosting model to predict daily $PM_{2.5}$ for 13 states in the northeastern USA. Other methods are based on chemical transport modelling using simulations of spatial-temporal varying scaling factors between AOD and PM (Van Donkelaar et al., 2010; Wang and Chen, 2016; Xu et al., 2015). Another category of methods are semi-empirical physical based models. They are more physically meaningful because they use an empirical relationship between AOD and $PM_{2.5}$ mass concentration and optical properties (Zhang et al., 2021) and incorporate key meteorological parameters (e.g. relative humidity, boundary layer height) to address the atmospheric influences on the AOD-PM relationship. Koelemeijer et al. (2006) and Di Nicolantonio et al. (2009) showed the suitability of these approaches for parts of Europe and especially for urban/industrial regions. Lin et al. (2015) estimated and incorporated main aerosol characteristics (mass extinction efficiency and size distribution) to their semi-empirical model to derive $PM_{2.5}$ concentrations for China. Tian and Chen (2010) employed additional meteorological parameters for their model and found a significant improvement in the model predictability for $PM_{2.5}$ concentrations in Southern Ontario (Canada) by considering surface temperature.

Among the many challenges in deriving $PM_{2.5}$ concentrations from AOD observations are variations in meteorological conditions, aerosol composition and the vertical distribution that can have strong effects on the PM-AOD relationship (Van Donkelaar et al., 2015). All mentioned methods have their advantages and disadvantages in taking these effects into account for an accurate derivation and prediction of $PM_{2.5}$ from satellite AOD.

Beside the applied model and environmental data input, the performance of estimated $PM_{2.5}$ concentrations also depends on the AOD data itself. Issues such as cloud contamination, heterogenous surface conditions or inaccurate retrievals can lead to uncertainties in the satellite-retrieved AOD values (Toth et al., 2014; Holzer-Popp et al., 2013). Furthermore, the availability of satellite data is limited to cloud-free conditions and certain overpass times (Christopher and Gupta, 2010). Many different AOD datasets were used for the estimation of ground-level $PM_{2.5}$ concentrations, all showing different results (see Chu et al., 2016). The most common AOD datasets applied for air quality studies are obtained from the Moderate Resolution Imaging Spectroradiometers (MODIS) onboard the Nasa satellites Terra and Aqua (Levy et al., 2007). Both, the original 10 km resolution MODIS AOD products and the more recent, recalculated products with 3 km spatial resolution were deployed and well proven in their suitability for air quality assessments. Especially the 3 km products offer high potential for regional pollution studies, as it provides more detail in spatial distribution of aerosols. However, the lifetime of MODIS is limited and its expected operation period is already exceeded (Yao et al., 2018). Next-generation satellites will replace the well-established instruments in future to continue the long-term data collection. A high potential candidate for global aerosol observations is the Sea and Land Surface Temperature Radiometer (SLSTR), which has been operating since 2017 onboard the ESA Copernicus Satellite Sentinel-3A (https://sentinel.esa.int/web/sentinel/user-guides/sentinel-3-slstr). To our knowledge SLSTR AOD data has not been used for studies on $PM_{2.5}$ derivation so far.

In this study we examine daily observations of AOD from three satellite sensors and apply a semi-empirical linear regression approach to derive surface $PM_{2.5}$ concentrations for Germany and parts of the surrounding countries. For the first time we therefore exploit a recent data set obtained from the Sentinel-3A/SLSTR instrument together with two well-established AOD data sets from the MODIS instruments on Terra and Aqua. With the ultimate goal to derive $PM_{2.5}$ concentrations for Germany at an area-wide coverage to examine the spatial distribution and to identify main aerosol sources, we analyse the satellite products with respect to data availability/coverage and their differences in AOD responses in collocated observations. Based on this analysis the observations are combined to an AOD ensemble to improve the representation of spatio-temporal aerosol variability. Using a semi-empirical linear regression approach, we evaluate the suitability and the benefit of the AOD ensemble to assess $PM_{2.5}$ concentrations.

Section 2 gives a detailed description of the data sets and of the method used for $PM_{2.5}$ derivation. Results of the comparison between the different AOD products are shown in Section 3, as well as the results for the $PM_{2.5}$ data set derived from the AOD ensemble product. Section 4 closes this study with a summary and discussion.

2. Methodology and data

2.1. Satellite-based $PM_{2.5}$ estimation

An accurate estimation of ground-level $PM_{2.5}$ concentrations depends on several factors. Beside the AOD data itself, the relationship between ground-level $PM_{2.5}$ and column integrated AOD depends on aerosol characteristics (e.g. composition, size, vertical distribution) and on meteorological conditions. For the derivation of ground-level $PM_{2.5}$ concentrations from satellite AOD, we use a semi-empirical approach based on the work of Koelemeijer et al. (2006) and Di Nicolantonio et al. (2009). This incorporates key meteorological parameters and presumes some physical knowledge to account for the aforementioned dependencies. The relationship between $PM_{2.5}$ and AOD can be written as:

$$PM_{2.5} = \tau \frac{4\,\rho\, r_{eff}}{3\,H\,f(RH)\,Q_{ext,dry}} \quad (1)$$

where τ is the satellite-derived AOD, ρ the particle density, r_{eff} the effective radius of aerosol particles, $Q_{ext,\ dry}$ the Mie-extinction efficiency at dry conditions, H the boundary layer height and RH the surface relative humidity.

The AOD is a measure of light extinction of the total atmospheric column. Without knowledge about the extinction profile, it is difficult to relate the AOD column measurements to surface level aerosol concentrations. Several studies have shown that the majority of aerosol particles is distributed in the lower troposphere and are vertically well mixed within the planetary boundary layer (Clarke et al., 1996; Kaufman et al., 2003; Sheridan and Ogren, 1999). Assuming the latter, we use the planetary boundary layer height (H) as approximation to account for the vertical profile of AOD in our approach. Relative humidity affects the water uptake process of aerosols and can cause changes in the aerosol size distribution, chemical composition and particle extinction properties (Liu et al., 2005). The function $f(RH)$ takes this so-called hygroscopic growth effect into account by describing the increase of the extinction cross-section of the aerosol by relative humidity (Koelemeijer et al., 2006). Following the work of Koelemeijer et al. (2006), we used an approximated function of RH based on nephelometer measurements by Veefkind et al. (1996). The parameters r_{eff}, $Q_{ext,\ dry}$ and ρ depend on aerosol composition and size distribution and can be classified by aerosol type. As the target region of our study is assumed to be dominated by only one aerosol type (urban industrial – weakly/non-absorbing), we use constant values for these parameters. The aerosol type specific values for these parameters are obtained from Levy et al. (2007a) and are consistent with the MODIS AOD retrieval.

To correct the $PM_{2.5}$ estimates for bias and scaling errors in comparison to in-situ ground measurements, we employ a linear regression approach. Regression parameters (slope and intercept) from linear regression between in-situ and satellite-derived $PM_{2.5}$ concentrations serve as correction factors. Due to spatially and temporally varying meteorological conditions, local emissions and aerosol chemical composition, the relationship between satellite-based and in-situ measured aerosol concentrations changes significantly with season and region (Gupta et al., 2006; Zhang et al., 2009). To consider these variations, correction factors were determined per station and month. Adding the correction factors to Eq. (1) gives the following regression formula:

$$PM_{2.5\,corrected} = A_{i,j} * PM_{2.5} + B_{i,j} \quad (2)$$

Factor A stands for the slope and factor B for the intercept parameter of the linear regression at station i and month j. Correction factors were calculated for all of the 350 stations, including all station types (background, industrial, traffic). The correction factors were interpolated to a 0.01° grid using an inverse distance weighting approach (Stachelek, 2014) to receive monthly correction maps for the mapping of $PM_{2.5}$ concentrations. To consider and estimate the model performance regarding model fitting, a 5-fold cross validation was performed. Therefore, we varied the stations considered for the interpolation of the correction parameters. We randomly split the station-wise data into five subsets of 70 stations and calculated five sets of correction parameters excluding one of the subsets respectively. We determined five different sets of $PM_{2.5}$ concentration data, which were then averaged to derive our final $PM_{2.5}$ dataset. For statistical analyzes we extracted the data collocated with station measurements, for the averaged final $PM_{2.5}$ data set (training data set) and for the 70 unconsidered stations of the five different $PM_{2.5}$ sets as test (validation) dataset.

To evaluate the model performance and to test for potential overfitting, statistical indicators such as root mean square error (RMSE), relative prediction error (RPE: RMSE divided by mean predicted $PM_{2.5}$) and the determination coefficient (R^2) were calculated for both, model and cross validation results.

2.2. Data sets

2.2.1. Satellite AOD data sets

In this study three different satellite AOD (550 nm) data sets were exploited. Two of them are based on measurements by the MOIDS instruments onboard the NASA satellites Terra and Aqua, the third is a recent dataset obtained from SLSTR instrument onboard Sentinel-3A Copernicus satellite. The satellite sensors and AOD products differ in terms of swath-width, overpass time, aerosol retrieval algorithms and resolution and will be briefly described below.

MODIS radiometers have been in operation since 2000 onboard Terra and since 2002 onboard Aqua, providing retrieval products of aerosol and cloud properties with global coverage every single or two days (Levy et al., 2007; Remer et al., 2005). Terra passes the equator around 10:30 local time in north-south direction, Aqua at 13:30 in south-north direction. The MODIS instruments measure spectral reflectance in 36 spectral bands from the solar to the thermal infrared with a swath width of 2330 km. For the aerosol retrieval, seven of these bands in the shortwave are used, and several others for the identification and masking of clouds. Different AOD retrieval algorithms are used for land and ocean surfaces in order to account for differences in surface reflectance and the types of aerosol

present (Rubin and Collins, 2014). The different retrieval algorithms are described in detail by Remer et al. (2006). For this study we used the new MODIS Collection 6.1 dark target AOD datasets with 3 km resolution from Aqua (MYD04_3K) and Terra (MOD04_3K) (Levy et al., 2013; Remer et al., 2013).

The SLSTR instrument is a dual-view imaging radiometer with a swath width of 1400 km in nadir view and 740 km in the along-track view. SLSTR collects reflectance data in nine spectral bands from 0.555 to 10.85 μm since the year 2017. There are several algorithms for the AOD retrieval, details can be found in (Popp, 2019). We used the 550 nm-AOD product with 10 km resolution based on the Swansea University Algorithm (North and Heckel, 2019). The dual-view method shows robust retrievals for both bright and dark surfaces. In contrast to single-view methods (e.g. MODIS), no a priori information on the surface albedo is required for the retrievals (Veefkind et al., 1998). This is a great advantage over MODIS where surface brightness exhibits a serious source of uncertainty in the AOD retrieval (Munchak et al., 2013; Remer et al., 2013). Sentinel-3A crosses the equator at 10:30 local time, matching the overpass time of Terra.

In order to pair up the AOD data with other data sets (meteorology and station data), we resampled the orbital AOD data (polygons) onto a fixed regular longitude latitude grid covering Germany and its direct surrounding (see Fig. 1). Following the study and recommendation of Sun et al. (2018) and the application of Müller et al. (2022) we use an output grid of $0.01^\circ \times 0.01^\circ$ for the tiling of the observations. For the given data this resolution is considered adequate to represent the information content of the irregular pixel polygons for any further averaging i.e. temporal aggregation procedure. We have not filtered the original AOD data based on any quality assurance flags and produced daily resampled AOD maps for each satellite product.

To improve the AOD coverage and data base for our analyses we combined the three data sets by averaging all available observations per pixel before deriving $PM_{2.5}$ concentrations. According to Guo et al. (2020) and Ma et al. (2014), we first extracted the pixel data, where all three products are available and performed a linear regression to obtain the relationship between the three products on a seasonal basis. We started matching up Aqua/MODIS and Terra/MODIS datasets by using this obtained linear relationship to predict the AOD values for grid cells where only one of the products is available. We then repeated the procedure matching up the combined MODIS product with SLSTR AOD. The pixel values of the final AOD product thus are averages of three different pixel values (per day). We call it combined AOD or rather ensemble.

2.2.2. *Ground-based $PM_{2.5}$ measurements*

The European Environment Agency (EEA) collects and publishes air quality data from in-situ measurement stations all across

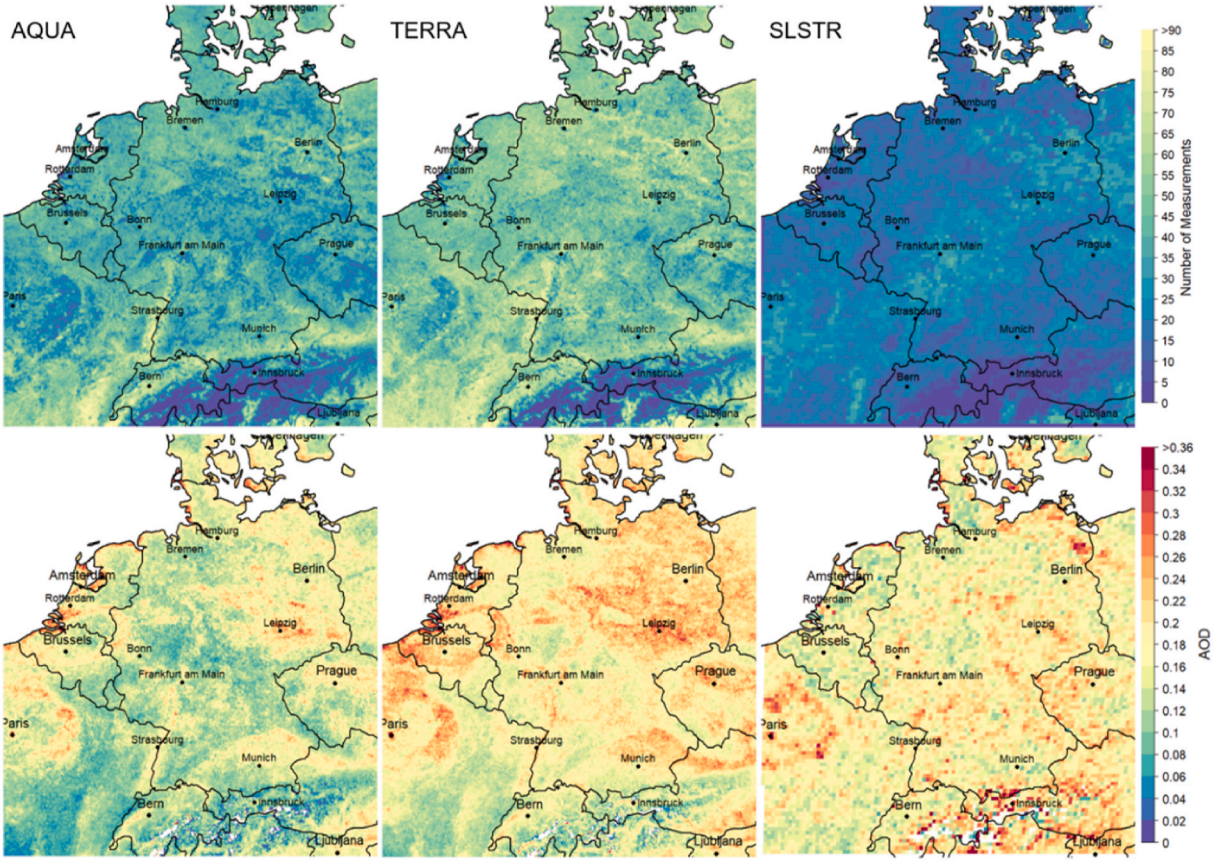

Fig. 1. Number of valid AOD retrievals (top) and mean AOD values (bottom) for the year 2018 derived from Aqua/MODIS, Terra/MODIS and SLSTR instruments.

Europe. The data for certain species can be downloaded per year and country at https://discomap.eea.europa.eu/map/fme/AirQualityExport.htm. Most of the stations provide up-to-date data on hourly basis (*E2a* data sets), but the completeness of the data differs significantly from station to station. For our study we use all available $PM_{2.5}$ measurements of the *E2a* data sets for the year 2018 and the region from 46°N to 56°N and 2°E to 16°E. This region comprises in total 350 stations in Germany (175), Poland (3), Czech Republic (32), Austria (24), Switzerland (1), France (54), Belgium (35), Luxembourg (4) and the Netherlands (24). We use daily mean $PM_{2.5}$ values per station in this study. Some stations already provide daily averages. For stations with hourly data, we calculated the daily average using all available measurements, when these consist of at least six hourly values.

2.2.3. Meteorological data

Meteorological data for Europe is provided by the European Centre for Medium-Range Weather Forecasts (ECMWF). We use the *Atmospheric Model high resolution 10-day forecast (Set*I - *HRES)* data set with 0.1° resolution for daily information on Boundary Layer Height (BLH) and Relative Humidity (RH) for the greater Germany region. The downloaded data sets include daily values for a single timestep (12am, matching the mean overpass time of the satellites) interpolated to a grid with 0.01 × 0.01° latitude-longitude spatial resolution.

3. Results

3.1. Comparison of Aqua/MODIS, Terra/MODIS and SLSTR

Three different AOD data sets were examined to eventually derive surface $PM_{2.5}$ concentrations over Germany and parts of the surrounding countries for the year 2018. As described above these datasets differ in terms of spatial resolution, the underlying AOD retrieval algorithm, overpass time and the sampling rate due to different swath-widths. While the MODIS datasets share the same retrieval algorithm and spatial resolution, they have a time difference in overpass of 3 h. The SLSTR data set is based on a dual-view mechanism and a different aerosol retrieval algorithm. It has a coarser resolution than the MODIS data sets, but shares the same overpass time with Terra/MODIS. Since a better understanding of the characteristics of the AOD observations is a prerequisite for our study, we first investigate the differences and similarities of the three satellite products.

3.1.1. AOD and coverage

Fig. 1 gives an overview on the absolute coverage (number of measurements) of the satellite products and the mean AOD distribution for the year 2018. In general, the MODIS data sets show higher numbers of measurements with averages of 39 ± 13 and 49 ± 15 measurements per grid cell for Aqua and Terra, respectively. This correspond to 10.7% and 13.4% of the possible daily measurements for one year. SLSTR provides 20 ± 9 measurements on average, which corresponds to 5.5% of all days. This can be mainly explained by the much smaller swath width of SLSTR, compared to the MODIS sensors. Each sensor exhibits spatial variations in the number of measurements which are more pronounced for the MODIS datasets with standard deviations for the mean number of measurements of 13 measurements for Aqua/MODIS and 15 measurements for Terra/MODIS compared to 9 measurements for SLSTR. The least covered region is the Alpine area due to snow cover and frequently cloudy conditions. In general, a correlation between the number of measurements and the orography was found. For example, the mountainous regions in central Germany show also lower number of measurements for all sensors. In addition, the low numbers of MODIS observations over optically bright surfaces, such as cities or agricultural areas, become obvious. Striking examples in this context are the city of Hamburg in northern Germany and the agricultural valley east of Paris. This demonstrates the algorithmic limitations of the applied MODIS products in this study and shows the advantage of the SLSTR dual-view mechanism and retrieval algorithm, as these surface dependent minima cannot be found in the SLSTR coverage.

Fig. 2 displays the total number of grid cells with AOD values per day for the year 2018 and reflects the differences in the daily

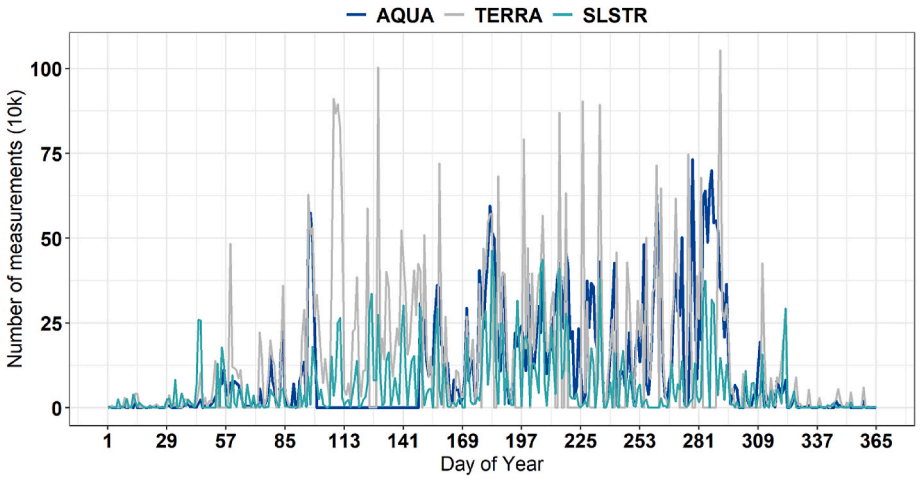

Fig. 2. Total daily number of AOD measurements for 2018 obtained from Aqua/MODIS, Terra/MODIS and SLSTR.

coverage between the three satellite sensors. Overall Terra/MODIS shows the best coverage with a maximum number of measurements for most of the days in 2018. On average, Terra/MODIS covers 10.2% of the study region each day compared to Aqua/MODIS and SLSTR with 7.8% and 4.3% mean daily coverage, respectively.

For all three sensors there are many days with no or very few measurements. Very pronounced is the gap in Aqua/MODIS data in May 2018 where technical issues prohibited data transmission. In general, all sensors have the lowest coverage in the winter season where weather conditions (snow cover) and the presence of clouds limit satellite measurements in the visual range. The timeseries shows (and comparisons of daily AOD maps which are not shown here) that Terra/MODIS and Aqua/MODIS are more similar in their day-by-day coverage than Terra/MODIS and SLSTR. This indicates a dominating influence of the swath-width and AOD-retrieval algorithm on the daily data availability compared to different overpass times i.e. temporal variability. Comparisons of daily AOD maps reveal that not only the daily number of measurements varies a lot but also the regions covered by these measurements. Thus, even when the satellite sensors i.e. the applied retrieval methods deliver the same number of pixels a day they can provide different spatial information.

The mean AOD values at 550 nm (Fig. 1) for 2018 show similar main patterns for MODIS and SLSTR throughout the area. Highest AODs can be found in eastern Germany and north-east of Paris with values mostly over 0.24. SLSTR and Terra/MODIS AODs are generally higher than that of Aqua/MODIS. SLSTR and Terra/MODIS have the same mean AOD value (0.18 ± 0.04), which is about 22% larger compared to that from Aqua/MODIS (0.14 ± 0.04). Median values are comparable to the mean values for all sensors. In general, gradients are clearer visible in the MODIS maps due to the better resolution. It is even possible to locate some isolated aerosol hotspots, like in the industrial area around Leipzig in eastern Germany. As the daily spatial information can differ significantly between the sensors and in particular between SLSTR and the MODIS products (Fig. 2), the differences in the annual mean maps can be misleading and are not necessarily related to differences in data quality or sensitivity. Therefore, we further analyzed the distributions and statistical characteristics of the data sets by only considering collocated measurements. The results of the comparison are depicted in Fig. 3 as violin plots and in Fig. 4 as timeseries of the monthly mean values for the collocated measurements. Table 1 moreover shows related statistical results for comparing the datasets quantitatively.

The violin plots of the AOD distributions, reveal a similar behavior for all three data sets. The distributions show the majority of AOD values in the lower range while the maxima are between 1.61 and 1.84. The unimodal distributions are skewed to the right with the median smaller than the mean and differ mainly for AOD <0.1. The inter quartile range is almost the same for all datasets with values of 0.16 for Aqua/MODIS and 0.15 for Terra/MODIS and SLSTR. The mean and medians are close (Table 1) with a maximum difference of 0.02 in median between SLSTR and Aqua/MODIS and in mean between Aqua/MODIS and Terra/MODIS considering all collocations in 2018. Differences in the annual mean maps though, seem to result from different daily information for the grid cells and not in differences of the sensor performances, as supposed before. Fig. 4 illustrates the monthly variation of mean AOD values for the three data sets. For most of the year, the mean values are very close to each other and lie within the standard deviations. Only in springtime higher deviations between SLSTR and the MODIS data sets can be observed. The best agreements between the datasets occur in summer and autumn.

From the above analysis, all data sets show comparable characteristics and can therefore all be used for $PM_{2.5}$ derivation. What is more, a combination of all three data sets could bring advantages with respect to coverage, resolution and sensitivity. For example, SLSTR has restrictions regarding coverage and spatial resolution, whereas MODIS delivers data in a higher spatial resolution with better daily coverage. On the other hand, MODIS data is limited over bright surfaces (e.g. cities) due to algorithmic limitations. It is hoped that this restriction can be at least partly reduced by using complementary SLSTR data. In the following we will therefore combine all three data sets to derive more complete and more reliable AOD maps.

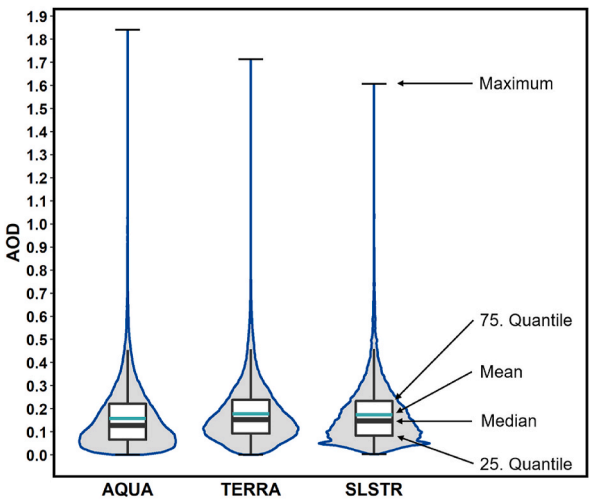

Fig. 3. Violin plots for all daily and spatially overlapping pixels (collocations) in 2018.

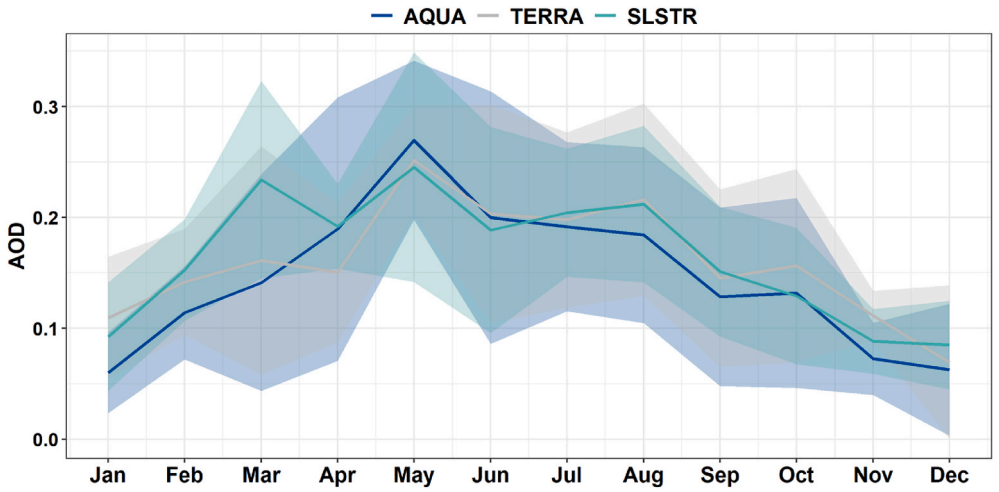

Fig. 4. Monthly mean AOD values for collocated observations of Aqua/MODIS, Terra/MODIS and SLSTR.

Table 1
Statistics based on collocations between AOD measurements of Aqua/MODIS, Terra/MODIS and SLSTR – Median, mean, standard deviation (STD) and number of collocations (N).

		2018	Spring	Summer	Autumn	Winter
Median	AQUA	0.13	0.15	0.14	0.09	0.06
	TERRA	0.15	0.17	0.16	0.12	0.09
	SLSTR	0.15	0.19	0.15	0.10	0.15
Mean	AQUA	0.16	0.17	0.17	0.12	0.07
	TERRA	0.18	0.18	0.19	0.14	0.10
	SLSTR	0.17	0.20	0.18	0.12	0.15
STD	AQUA	0.12	0.12	0.13	0.11	0.05
	TERRA	0.12	0.11	0.13	0.10	0.06
	SLSTR	0.12	0.11	0.13	0.08	0.07
N		3456216	553797	2301938	575950	24521

3.1.2. AOD ensemble

For the combination of the AOD data sets we averaged all daily available AOD values from the completed AOD data set (see regression procedure in section 2.2.1) for the target region. We have not filtered or weighted the data sets for this calculation, as we are not able to quantify which dataset is the closest to the truth. As tentative quality measure we rely on the absolute differences in the monthly mean AOD values (Fig. 4). Total difference means here, we consider the maximum difference per day, independent from the dataset providing the minimum or maximum value. The mean monthly, seasonal and annual differences are presented in Fig. 5. As discussed in the previous section, the differences are in general not extensive, with a mean annual difference of about 0.07. The only season with differences over 0.1 were found for spring-time and in particular the months of March and April.

On average, the ensemble product covers 16.7% of the study region each day which is nearly twice the daily coverage of the

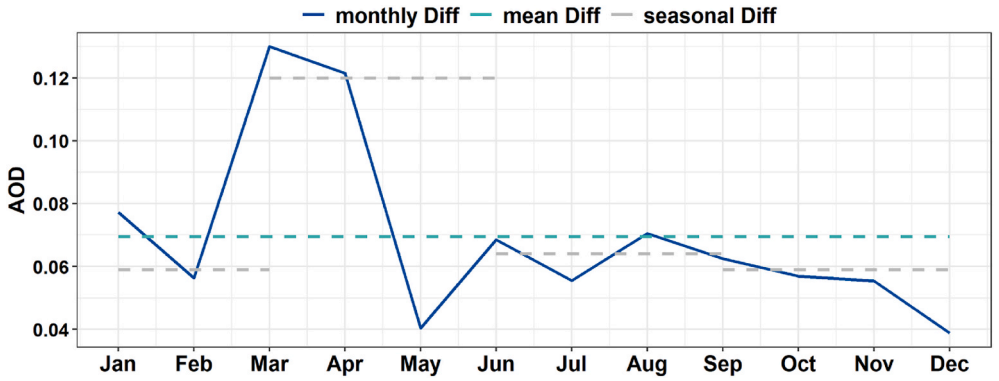

Fig. 5. Absolute differences between daily collocated mean AOD values on annual, seasonal and monthly basis.

individual products. Maps of seasonal mean AOD distributions are depicted in Fig. 6. Thanks to the consideration of all available observations in the combined data set, the maps are almost completely covered, i.e. by more than 96% in spring, summer and autumn. Only in the winter period with a coverage of 76% there are still larger gaps. An annual cycle can be observed in the AOD distributions, with higher values in spring and summer. Corresponding mean AOD values are 0.19 ± 0.03 and 0.21 ± 0.03 for spring and summer, respectively, compared to 0.12 ± 0.02 for autumn and 0.15 ± 0.05 for the winter season. Strongest spatial variation can be found for winter with a standard deviation of 0.05. The regions with higher aerosol load in the East and near Paris, which could be identified in the annual mean maps (Fig. 1), can be found in all seasons, but are more extensive in spring and autumn.

3.2. Ground-level $PM_{2.5}$ concentrations

Based on the combined AOD data set daily $PM_{2.5}$ data sets were generated. As described in section 2.1 we first derived $PM_{2.5}$ concentrations using the physical relationship given in equation (1) and corrected it in a second step for seasonal and location specific bias and scaling errors using in-situ measurements. To highlight the effect of correction by in-situ measurements, Fig. 7 shows hexbin plots between in-situ and satellite-derived PM values before and after the correction. Table 2 gives the corresponding statistical assessment. We included all collocations between stations and satellite measurements for the year 2018.

PM values directly derived from satellite AOD show strong overestimations compared to in-situ data with a bias of 26.3 μg/m^3, and the correlation with station measurements is rather low with an R-value of 0.31. After the correction the bias is reduced significantly (0.2 μg/m^3), but stays positive, indicating that the satellite based $PM_{2.5}$ values are on average still a bit higher than the in-situ-measurements. The scatterplot shows, that the corrected $PM_{2.5}$ values are a bit more underestimated in the higher value range after the correction. Anyway, the overall agreement with in-situ data is strongly improved. We now obtain a correlation coefficient of 0.76. Mean and median values are reduced by more than 60% and also standard deviation and RMSE are strongly reduced by the

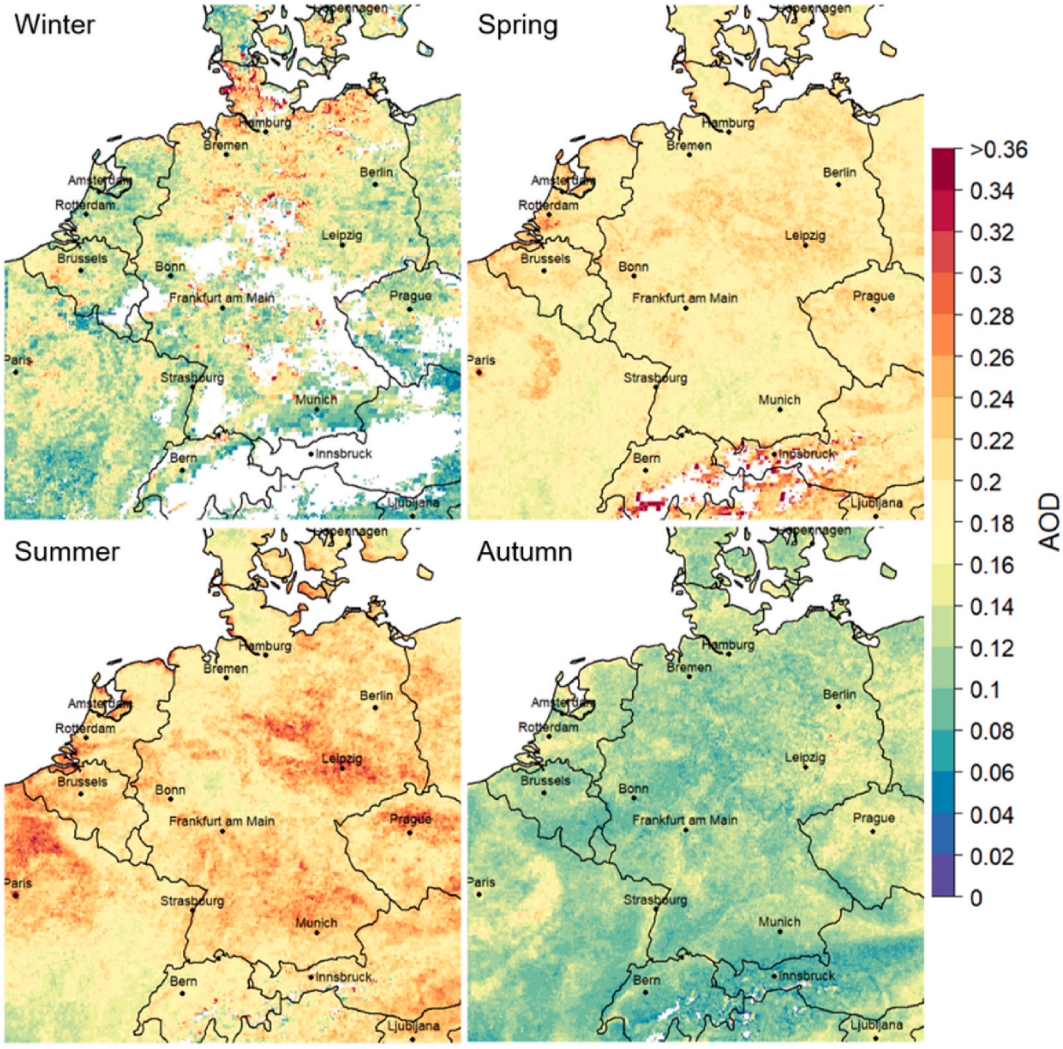

Fig. 6. Seasonal mean AOD maps based on the AOD ensemble product for 2018.

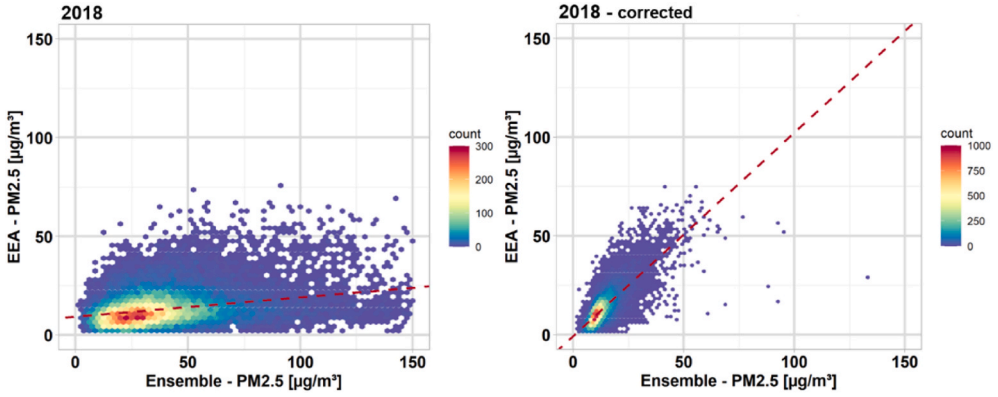

Fig. 7. Hexbin plots between in-situ (EEA) and satellite-based (Ensemble) $PM_{2.5}$ before (left) and after (right) the correction including all collocations for the year 2018.

Table 2
Statistics based on collocations between in-situ (EEA) and satellite-based (SAT) $PM_{2.5}$ concentrations before and after the correction and for the independent validation data set. Number of collocations (N), correlation coefficient (R), root mean square error (RMSE), bias, determination coefficient (R^2), relative prediction error (RPE), mean, median and standard deviation (Std).

	N	R	RMSE µg/m^3	Bias µg/m^3	R^2	RPE %	Mean SAT µg/m^3	Std SAT µg/m^3	Median SAT µg/m^3	Mean EEA µg/m^3	Std EEA µg/m^3	Median EEA µg/m^3
$PM_{2.5}$												
2018	26168	0.31	36.3	26.3	0.09	91.9	39.5	26.3	33.2	13.2	8.3	11.5
Winter	1328	0.28	25.9	15.2	0.08	74.6	34.7	21.1	30.7	19.6	11.6	17.6
Spring	6797	0.34	37.3	29.2	0.12	84.8	44.0	24.8	37.9	14.8	8.9	13.0
Summer	9943	0.25	40.5	29.5	0.06	103.	39.5	28.6	31.8	9.9	4.9	9.7
Autumn	8100	0.46	31.1	21.8	0.21	85.2	36.5	24.9	30.9	14.7	9.1	12.6
$PM_{2.5}$ corrected												
2018	26168	0.76	5.5	0.2	0.57	41.4	13.3	6.1	11.7	13.2	8.3	11.5
Winter	1328	0.62	9.1	−0.3	0.39	47.2	19.3	7.9	18.6	19.6	11.6	17.6
Spring	6797	0.71	6.2	0.1	0.51	41.6	14.9	6.3	13.4	14.8	8.9	13.0
Summer	9943	0.65	3.8	0.3	0.42	37.3	10.2	2.7	10.0	9.9	4.9	9.7
Autumn	8100	0.78	5.7	0.3	0.60	38.3	14.9	6.8	13.3	14.7	9.1	12.6
$PM_{2.5}$ corrected - validation												
2018	26168	0.65	6.4	0.4	0.42	47.0	13.5	5.6	11.8	13.2	8.3	11.5
Winter	1328	0.48	10.2	−0.9	0.23	54.5	18.7	6.5	18.3	19.6	12.0	17.6
Spring	6797	0.58	7.3	0.3	0.34	48.3	15.1	5.9	13.4	14.8	8.9	13.0
Summer	9943	0.4	4.5	0.4	0.16	43.3	10.4	2.2	9.9	9.9	4.9	9.7
Autumn	8100	0.69	6.6	0.5	0.48	43.4	15.2	6.0	13.7	14.7	9.1	12.6

correction. Before the correction our model could explain only about 10% of the variability in the in-situ measurements, after performing the correction our model can explain 57% of the variability. This is a significant improvement.

What is more, the seasonal statistics have also improved with the correction of the model in terms of bias, correlation and RMSE. The seasonal correlations with in-situ data are between 0.62 in winter and 0.78 in autumn. Especially interesting is the change in the bias for the winter season. The negative bias after the model correction indicates an overcorrection of the $PM_{2.5}$ concentrations in winter. This can be explained by the very small sample size for the station-wise linear regression procedure. For January and December there are even less than 10 stations for which the correction parameters could be calculated, leading to higher uncertainties in the interpolated correction maps. In summer the correlation is lower and the bias is higher, compared to spring, while the sample size in summer is higher. This suggests, that there are more measurements in summer that were not properly corrected. The satellite-based mean $PM_{2.5}$ concentrations are between 10.2 ± 2.7 µg/m^3 in summer and 19.3 ± 7.9 µg/m^3 in winter, whereas standard deviation in winter is almost three times higher than in summer. This can maybe be attributed to the number of collocations. Higher standard deviations seem to be correlated with lower numbers of collocations (see Table 2).

Validation results are also given in Table 2. Correlations are by 0.12 lower for the validation data set than for the final data set, indicating a weaker performance of our model for independent data. The mean values of the predicted $PM_{2.5}$ concentrations are comparable between test and training data sets, medians are even almost the same for all seasons. R^2 is 26% lower for the validation data set with a value of 0.42 compared to 0.57 for the complete year 2018. At the same time RMSE and RPE are with 6.4 µg/m^3 and 47% higher for the validation data set. This indicates that our model is slightly overfitted.

Fig. 8 shows the seasonal mean maps of the corrected satellite-based $PM_{2.5}$ concentrations. The $PM_{2.5}$ distributions look slightly different compared to the AOD distributions. Still high polluted areas are visible, but we can also see some seasonal anti-correlations between AOD and $PM_{2.5}$. The most striking example is the summer season. Fig. 6 showed maximum AOD values for this season, but

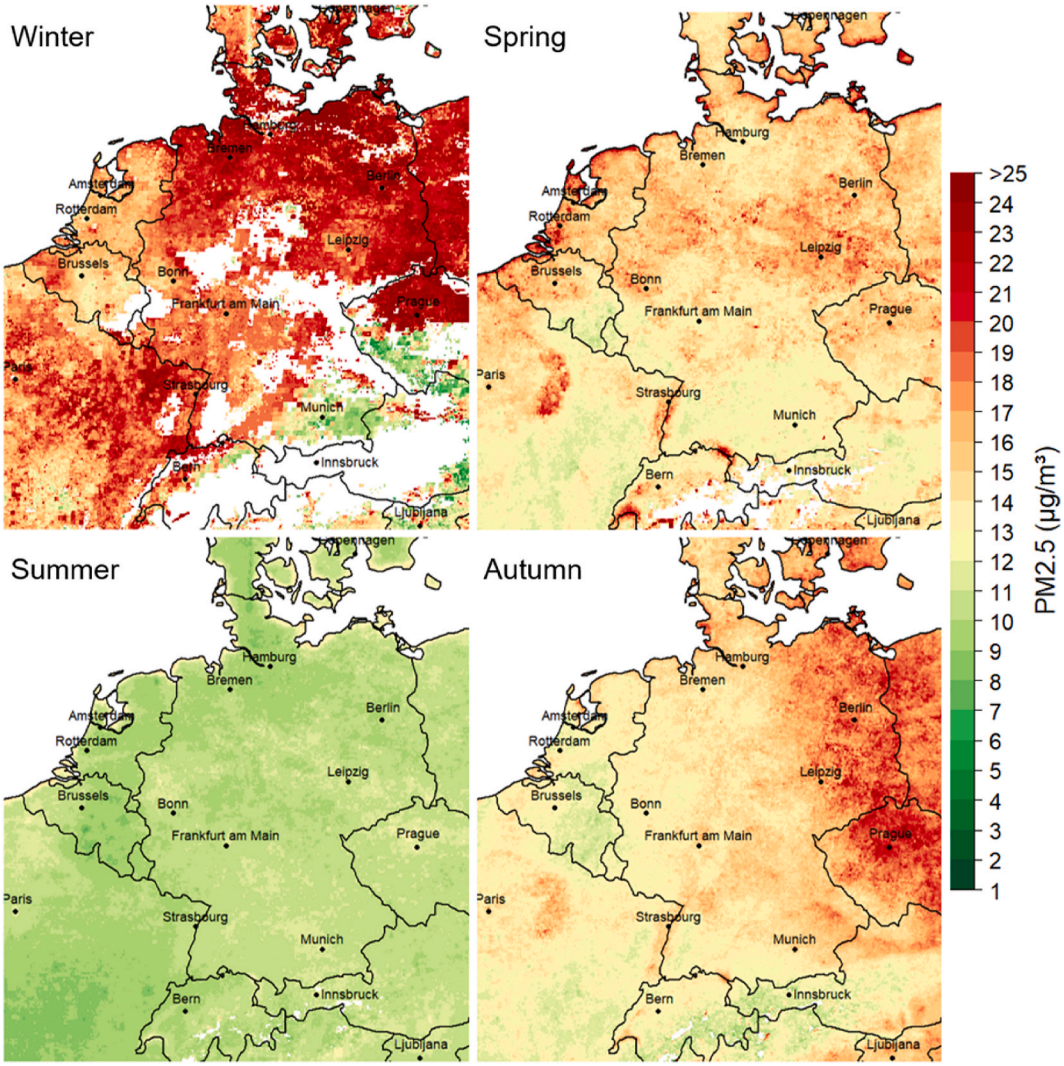

Fig. 8. Seasonal mean $PM_{2.5}$ concentrations (corrected) derived from the AOD ensemble product for 2018.

ground-level $PM_{2.5}$ concentrations have their minimum in summer. This anticorrelation is caused by the consideration of the boundary layer height as a vertical measure of the aerosol distribution. In Europe, the boundary layer extension is usually much higher in summer than in the cold season (Seidel et al., 2012). As we assume a homogeneous vertical mixing of the aerosol along the full vertical extend of the boundary layer, higher AOD values result in lower ground-level $PM_{2.5}$ concentrations in summer. On the contrary, in the cold season where the boundary layer is rather flat, high AOD values result in even higher $PM_{2.5}$ concentrations.

Overall the $PM_{2.5}$ maps in Fig. 8 enable an overview on the seasonal amount and transnational distribution of fine aerosol particles near the surface. In winter we find in general the highest $PM_{2.5}$ concentrations over most areas with a mean value of 18.7 ± 4.3 µg/m^3 compared to 14.6 ± 2.0 µg/m^3, 10.3 ± 0.8 µg/m^3 and 14.7 ± 2.4 µg/m^3 for spring summer and autumn, respectively. We assume that these are mainly caused by heating activities in the cold season. In spring the region east of Paris is one of the most polluted areas. It is especially dominated by agricultural emissions and is a leader region for mineral fertilization causing high $PM_{2.5}$ concentrations from March to August (Viatte et al., 2020). Moreover, the orography can cause an accumulation of aerosol in valleys.

In autumn, eastern Germany, Poland and Czech Republic are higher polluted. These areas are also strongly impacted by agricultural emissions which may explain the observed pattern (Lelieveld et al., 2015). Long-range transport from sources in eastern Europe can be another explanation.

Annual mean $PM_{2.5}$ concentrations for 2018 are presented in Fig. 9. Due to the small number of measurements, the winter season has a very small contribution to the annual mean $PM_{2.5}$ pattern. The annual $PM_{2.5}$ values range from 7.9 µg/m^3 to 28.9 µg/m^3 with a mean value of 13.1 ± 1.4 µg/m^3. The dots in Fig. 9 present station wise correlations including all collocations for the year 2018. Overall the correlations are satisfactory, especially in the eastern part of the target region, where the coverage is comparatively good (see Fig. 1). We cannot find a systematic behavior regarding the geo-specific performance of our approach. On the other hand, for some

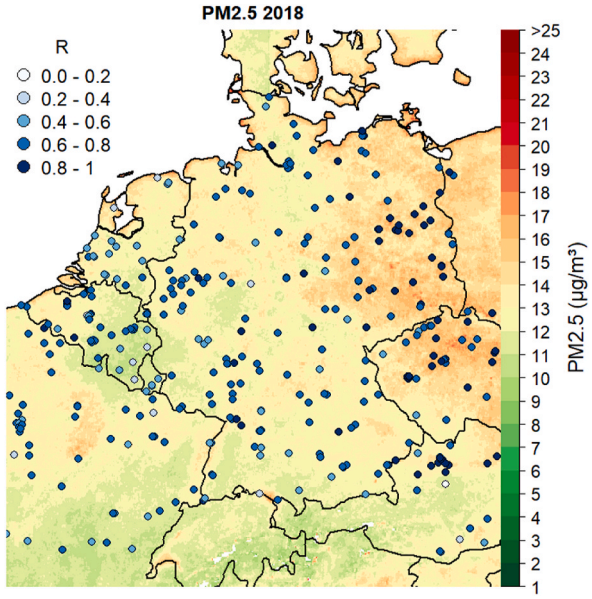

Fig. 9. Mean $PM_{2.5}$ concentration (corrected) for the year 2018 derived from the AOD ensemble product. The colored dots show station wise correlations between the satellite-based and in-situ measured $PM_{2.5}$ concentrations.

regions, correlations are significantly lower, for example, in the Netherlands and the area around Luxembourg. These areas are maybe dominated by specific aerosol types which are not well reproduced with our method (e.g. higher portion of sea salt aerosol). Overall, the good agreement between the estimated and in-situ measured $PM_{2.5}$ concentrations supports the main assumptions of our approach and demonstrates that ground-level $PM_{2.5}$ concentrations can be successfully derived from the 3-sensor AOD ensemble.

4. Summary and discussion

We examined the differences and similarities of collocated AOD footprints from Terra/MODIS, Aqua/MODIS and SLSTR on a daily basis and could show a similar behavior of all three datasets. All data sets have their advantages and disadvantages in terms of coverage, resolution and algorithmic performance. The MODIS sensors have provided reliable aerosol retrievals for decades and are still operational. However, its predicted operation time is already exceeded and the sensors underlie some instrumental degradation, causing a decline of data quality over time (Lyapustin et al., 2014; Yao et al., 2018). Although the AOD retrieval algorithms have been improved with Collection 6, this instrumental degradation cannot be eliminated completely. The new SLSTR sensor has provided high quality AOD observations since 2017. However, compared to MODIS, the SLSTR AOD product is currently more limited with respect to spatial resolution (10 km) and coverage due to the smaller swath width. MODIS data on the other hand, have a higher spatial resolution (3 km) and a considerably better daily coverage. However, a drawback of MODIS based dark target retrievals is their limited availability over bright surfaces (e.g. cities). Consequently, we tried to compensate the individual disadvantages by combining the three AOD datasets. This way we kept the positive characteristics of all three datasets and produced a better quality and more complete AOD data set with adequate resolution and increased overall coverage. Quantitatively, we could improve the mean daily coverage of 10.2% at maximum by the individual sensors to 16.7% for the ensemble product.

We investigated the performance of a semi-empirical linear regression approach for the estimation of national-scale $PM_{2.5}$ concentrations for Germany and surrounding countries using the three sensor AOD ensemble. To account for the influence of vertical structure and hygroscopic growth effect on the relationship between columnar AOD and near-surface $PM_{2.5}$, AOD values were coupled with meteorological parameters (RH, BLH) to derive ground-level $PM_{2.5}$ concentrations. Furthermore, in-situ measurements were used for linear regression to correct the derived $PM_{2.5}$ values for bias and scaling errors. With this correction, correlations between satellite and in-situ data sets could be strongly improved and errors (bias, RMSE) significantly reduced. We received high correlations with in-situ data of 0.76, a bias of 0.2 $\mu g/m^3$ and a RMSE of 5.5 $\mu g/m^3$ accounting for the entire year 2018 and could produce $PM_{2.5}$ maps with adequate coverage and a spatial resolution which could be highly valuable for regional air quality assessments.

Most comparable previous studies on deriving PM from satellite AOD used MODIS AOD data with a resolution of 10 km. Depending on the method they showed a wide range of R-values between 0.2 and 0.97 for different time periods and regions (Chu et al., 2016). Tian and Chen (2010) applied a semi-empirical model, to derive $PM_{2.5}$ concentrations in Canada. They found correlations of 0.65 using MODIS data with 10 km resolution. Also, Di Nicolantonio et al. (2009) used a semi-empirical approach on Aqua/MODIS 10 km AOD leading to a correlation of 0.59 between measured and satellite-derived $PM_{2.5}$ for Northern Italy.

Our results for Germany, using the higher resolution MODIS datasets combined with the 10 km resolution SLSTR product, in general exceed these performances, which is in line with several studies using better-resolved AOD data. Xie et al. (2015) showed an improvement in correlations using the 3 km Aqua/MODIS data set for urban-scale PM studies in Beijing, China. Mei et al. (2019)

investigated the effect of AOD resolution on the AOD-PM relationship for different regions in the US and found a positive effect on correlations when using higher resolution AODs for several spatial scales ranging from urban to continental scale. Also, Chudnovsky et al. (2013a) showed an increased correlation between AOD and $PM_{2.5}$ concentrations with increased spatial resolution in the USA. The results demonstrate the benefit of the MODIS 3 km AOD products for air quality studies on urban and regional scales, because it provides much more detail in spatial variability. Wu et al. (2019) analyzed the AOD-$PM_{2.5}$ relationship at spatial scales ranging from 40 m to 5 km in China. They found that correlations are generally higher at finer spatial scales in a range between 1 km and 5 km. On scales smaller than 1 km correlations fluctuated irregularly which they attributed to scale mismatches between AOD and $PM_{2.5}$ measurements. These results reveal, that the benefit of higher resolution AOD products for $PM_{2.5}$ estimations prevail only at a certain range, i.e. between 3 km and 1 km spatial resolution.

In general, the quality of the AOD data has a strong effect on the quality of PM estimates. Both, the accuracy of the retrieval algorithms and the amount of sampling data play a role. The accuracy of an aerosol retrieval algorithm is linked to the ability to decouple individual aerosol and surface contributions to the top of atmosphere reflectance observed by the satellite sensor (Holzer-Popp et al., 2013; Mei et al., 2019). Algorithmic limitations of the retrieval of AOD over bright and highly reflective surfaces (e.g. urban and agricultural areas, coastal regions) cause less reliability in contrast to AOD retrievals over dark surfaces (Sorek-Hamer et al., 2015) for most of the common satellite sensors. Dark target algorithms make use of reflectance differences between the aerosol and the underlying surface by assuming a dark surface (Levy et al., 2013). Over bright surfaces this assumption is not applicable and the algorithms fail. The MODIS 3 km AOD products are especially affected by this issue (see Munchak et al., 2013; Remer et al., 2013). Hence, accuracy and amount of MODIS AOD data is reduced over brighter surfaces and we could clearly observe the latter effect in our study (Fig. 1). Here, dual-view instruments like SLSTR have a significant advantage, because uncertainties due to the underlying surface brightness are reduced. The dual-view capability of the instrument allows AOD estimation without a priori assumptions on surface spectral reflectance, like “dark targets” (North and Heckel, 2019; Popp, 2019). With the combination of the AOD datasets we tried to compensate for this drawback of the MODIS datasets by adding the SLSTR data set which contains appropriate information for those regions where MODIS data is limited.

One critical point about our method to derive surface $PM_{2.5}$ concentrations is the station- and month-wise calculation of the correction parameters. On the one hand, this is a good practice to reproduce the spatial and temporal variation of local aerosol sources and meteorological conditions which affect the AOD-PM relationship. On the other hand, the quality and representativeness of the calculations strongly depend on the amount of data available per month and station. Although we could improve the database for the linear regression procedure by using the AOD ensemble product, there are still some time periods and locations, where lacks of the data base considerably reduce the quality of the correction parameters and thus of the resulting $PM_{2.5}$ values.

Another critical point about our method is the assumption of a single aerosol type. Although, it is matching the aerosol type used for the MODIS AOD retrieval for the target region (Levy et al., 2007a), aerosols can vary significantly with season and region (Putaud et al., 2004). In fact, we clearly see a seasonal variation in the correlations, which could be an indication of changing aerosol type. However, although Germany can be clearly separated in regions with different background conditions due to locally dominating emission sources (urban and coastal areas, mountainous and industrial regions, etc.), we do not find too much spatial variation in the accuracy of $PM_{2.5}$ estimates. Overall, we conclude that the spatial variation of aerosol composition and size does not have an important effect for monthly $PM_{2.5}$ aggregations over Germany, and that our assumption of a constant (urban-industrial) aerosol type is in general valid. In addition, we assume that our seasonal and location-specific correction method compensates to a certain extent for possible effects of aerosol-type variation within the country.

An exception was found for great parts of the Netherlands where correlations between the estimated and measured $PM_{2.5}$ concentrations were considerably lower compared to the rest of the study region. Schaap et al. (2009) found an important influence of aerosol type on the AOD-PM relationship in the Netherlands, due to strongly varying contributions of sea salt to the total aerosol mass in different parts of the country. We thus conclude, that our assumption of constant aerosol type is especially not valid for regions, with high portions of sea salt like the North Sea.

Other studies revealed a much more important effect of regionally differing aerosol types and climatic conditions on AOD-PM relationships. For the USA, e.g. Al-Saadi et al. (2005) found a large variation between the eastern and western part of the country. These regions strongly differ regarding aerosol composition and climatic conditions.

Although the results of our study are promising so far, we found some drawbacks in the application of our method to derive $PM_{2.5}$ surface concentrations from AOD and see room for improvement. The inclusion of additional meteorological parameters, such as surface temperature and wind, land use information or population related parameters could bring further improvement (e.g. Kloog et al., 2015; Zheng et al., 2016). The use of a linear mixed effects model, would allow the simultaneous consideration of these different kinds of variables for the linear regression using the whole data set(s) not split for month or season. Yao et al. (2018), You et al. (2015) and Liu et al. (2007) for example received good results using mixed effects models over China and the US. Furthermore, consideration of how the vertical distribution of aerosols affects the AOD-$PM_{2.5}$ relationship should be taken in to account in further studies. Therefore, one could use simulations from chemistry-transport models, as was done in a recent study by Yao and Palmer (2021), who used statistical and machine learning methods to model AOD-$PM_{2.5}$ relationships for China.

As mentioned before, the next-generation satellite sensors like SLSTR or VIIRS will take over the role of more established sensors like MODIS in the future and will allow to continue long-term global observations (Levy et al., 2015). As a follow-up we would like to investigate the performance of a linear mixed effects model for the SLSTR and MODIS AOD product separately and examine the sensitivity of different parameters to attain high-quality $PM_{2.5}$ retrievals from SLSTR and MODIS AOD data.

Since we considered one year of data only, the results may not be statistically representative for a longer period. However, we demonstrated the potential of a combined AOD product from different satellite sensors and retrieval algorithms for the derivation of

ground level $PM_{2.5}$ concentrations. We were able to produce reliable $PM_{2.5}$ concentration maps for Germany in a sufficient resolution which could be highly valuable for regional air quality assessments.

Funding

This work was supported by mFUND program of the Federal Ministry for Digital and Transport (BMDV) for project S-VELD [grant no. 19F2065] and partially by the Bavarian Ministry for Environment and Consumer Protection project JOSEFINA [grant no. 70606].

Author contributions

JH, TE, FB and MS designed the research and conceived the analysis. JH collected and processed the data. JH analyzed the data and wrote the manuscript. TE and FB contributed to the interpretation of the results. All authors provided critical feedback and helped to edit and improve the manuscript.

Declaration of competing interest

The authors declare that they have no known competing financial interests or personal relationships that could have appeared to influence the work reported in this paper.

Acknowledgement

We are grateful to all data suppliers. We would especially thank NASA for providing MODIS AOD data and Swansea University (Dr. Peter North and colleagues), who processed as part of the Copernicus Climate Change Service the 10 km SLSTR AOD product we used. SLSTR belongs to the new European Sentinel satellites supported by the Copernicus program. In-situ $PM_{2.5}$ data was provided by the European Environmental Agency, data of boundary layer height and relative humidity by ECMWF. Last but not least we want to thank the Editor and the Reviewers for their constructive comments to strengthen the manuscript.

References

Al-Saadi, J., Szykman, J., Pierce, R.B., Kittaka, C., Neil, D., Chu, D.A., et al., 2005. Improving national air quality forecasts with satellite aerosol observations. Bull. Am. Meteorol. Soc. 86 (9), 1249–1262.

Beelen, R., Raaschou-Nielsen, O., Stafoggia, M., Andersen, Z.J., Weinmayr, G., Hoffmann, B., et al., 2014. Effects of long-term exposure to air pollution on natural-cause mortality: an analysis of 22 European cohorts within the multicentre ESCAPE project. Lancet 383 (9919), 785–795.

Beloconi, A., Kamarianakis, Y., Chrysoulakis, N., 2016. Estimating urban PM10 and PM2. 5 concentrations, based on synergistic MERIS/AATSR aerosol observations, land cover and morphology data. Rem. Sens. Environ. 172, 148–164.

Beloconi, A., Chrysoulakis, N., Lyapustin, A., Utzinger, J., Vounatsou, P., 2018. Bayesian geostatistical modelling of PM10 and PM2. 5 surface level concentrations in Europe using high-resolution satellite-derived products. Environ. Int. 121, 57–70.

Chen, G., Li, S., Knibbs, L.D., Hamm, N.A., Cao, W., Li, T., et al., 2018. A machine learning method to estimate PM2. 5 concentrations across China with remote sensing, meteorological and land use information. Sci. Total Environ. 636, 52–60.

Christopher, S.A., Gupta, P., 2010. Satellite remote sensing of particulate matter air quality: the cloud-cover problem. J. Air Waste Manag. Assoc. 60 (5), 596–602.

Chu, Y., Liu, Y., Li, X., Liu, Z., Lu, H., Lu, Y., et al., 2016. A review on predicting ground PM2. 5 concentration using satellite aerosol optical depth. Atmosphere 7 (10), 129.

Chudnovsky, A., Lyapustin, A., Wang, Y., Schwartz, J., Koutrakis, P., 2013. Analyses of high resolution aerosol data from MODIS satellite: a MAIAC retrieval, southern New England, US. In: First International Conference on Remote Sensing and Geoinformation of the Environment (RSCy2013), 8795. International Society for Optics and Photonics, p. 87951E.

Chudnovsky, A.A., Kostinski, A., Lyapustin, A., Koutrakis, P., 2013a. Spatial scales of pollution from variable resolution satellite imaging. Environ. Pollut. 172, 131–138.

Clarke, A.D., Porter, J.N., Valero, F.P.J., Pilewskie, P., 1996. Vertical profiles, aerosol microphysics, and optical closure during the Atlantic Stratocumulus Transition Experiment: measured and modeled column optical properties. J. Geophys. Res. Atmos. 101 (D2), 4443–4453.

Di Nicolantonio, W., Cacciari, A., 2011. MODIS multiannual observations in support of air quality monitoring in Northern Italy. Italian J. Rem. Sensing/Rivista Italiana di Telerilevamento 43 (3).

Di Nicolantonio, W., Cacciari, A., Tomasi, C., 2009. Particulate matter at surface: northern Italy monitoring based on satellite remote sensing, meteorological fields, and in-situ samplings. IEEE J. Sel. Top. Appl. Earth Obs. Rem. Sens. 2 (4), 284–292.

Engel-Cox, J.A., Holloman, C.H., Coutant, B.W., Hoff, R.M., 2004. Qualitative and quantitative evaluation of MODIS satellite sensor data for regional and urban scale air quality. Atmos. Environ. 38 (16), 2495–2509.

European Environment Agency, 2021. Air Quality in Europe 2021, Report No. 15/2021. Air Quality in Europe 2021 — European Environment Agency (europa.eu).

Fang, X., Zou, B., Liu, X., Sternberg, T., Zhai, L., 2016. Satellite-based ground PM2. 5 estimation using timely structure adaptive modeling. Rem. Sens. Environ. 186, 152–163.

Guo, H., Li, W., Yao, F., Wu, J., Zhou, X., Yue, Y., Yeh, A.G., 2020. Who are more exposed to PM2. 5 pollution: a mobile phone data approach. Environ. Int. 143, 105821.

Gupta, P., Christopher, S.A., Wang, J., Gehrig, R., Lee, Y.C., Kumar, N., 2006. Satellite remote sensing of particulate matter and air quality assessment over global cities. Atmos. Environ. 40 (30), 5880–5892.

He, Q., Huang, B., 2018. Satellite-based mapping of daily high-resolution ground PM2. 5 in China via space-time regression modeling. Rem. Sens. Environ. 206, 72–83.

Hoff, R.M., Christopher, S.A., 2009. Remote sensing of particulate pollution from space: have we reached the promised land? J. Air Waste Manag. Assoc. 59 (6), 645–675.

Holzer-Popp, T., Leeuw, G.D., Griesfeller, J., Martynenko, D., Klüser, L., Bevan, S., et al., 2013. Aerosol retrieval experiments in the ESA Aerosol_cci project. Atmos. Meas. Tech. 6 (8), 1919–1957.

Hu, X., Waller, L.A., Al-Hamdan, M.Z., Crosson, W.L., Estes Jr., M.G., Estes, S.M., et al., 2013. Estimating ground-level PM2. 5 concentrations in the southeastern US using geographically weighted regression. Environ. Res. 121, 1–10.

Just, A.C., Arfer, K.B., Rush, J., Dorman, M., Shtein, A., Lyapustin, A., Kloog, I., 2020. Advancing methodologies for applying machine learning and evaluating spatiotemporal models of fine particulate matter (PM2. 5) using satellite data over large regions. Atmos. Environ. 239, 117649.

Kacenelenbogen, M., Léon, J.F., Chiapello, I., Tanré, D., 2006. Characterization of aerosol pollution events in France using ground-based and POLDER-2 satellite data. Atmos. Chem. Phys. 6 (12), 4843–4849.

Kaufman, Y.J., Haywood, J.M., Hobbs, P.V., Hart, W., Kleidman, R., Schmid, B., 2003. Remote sensing of vertical distributions of smoke aerosol off the coast of Africa. Geophys. Res. Lett. 30 (16).
Khomenko, S., Cirach, M., Pereira-Barboza, E., Mueller, N., Barrera-Gómez, J., Rojas-Rueda, D., et al., 2021. Premature mortality due to air pollution in European cities: a health impact assessment. Lancet Planet. Health 5 (3), e121–e134.
Kloog, I., Ridgway, B., Koutrakis, P., Coull, B.A., Schwartz, J.D., 2013. Long-and short-term exposure to PM2. 5 and mortality: using novel exposure models. Epidemiology 24 (4), 555–561.
Kloog, I., Sorek-Hamer, M., Lyapustin, A., Coull, B., Wang, Y., Just, A.C., et al., 2015. Estimating daily PM2. 5 and PM10 across the complex geo-climate region of Israel using MAIAC satellite-based AOD data. Atmos. Environ. 122, 409–416.
Koelemeijer, R.B.A., Homan, C.D., Matthijsen, J., 2006. Comparison of spatial and temporal variations of aerosol optical thickness and particulate matter over Europe. Atmos. Environ. 40 (27), 5304–5315.
Kumar, N., Liang, D., Comellas, A., Chu, A.D., Abrams, T., 2013. Satellite-based PM concentrations and their application to COPD in Cleveland, OH. J. Expo. Sci. Environ. Epidemiol. 23 (6), 637–646.
Lai, H.K., Tsang, H., Thach, T.Q., Wong, C.M., 2014. Health impact assessment of exposure to fine particulate matter based on satellite and meteorological information. Environ. Sci.: Processes & Impacts 16 (2), 239–246.
Lelieveld, J., Evans, J.S., Fnais, M., Giannadaki, D., Pozzer, A., 2015. The contribution of outdoor air pollution sources to premature mortality on a global scale. Nature 525 (7569), 367–371.
Lelieveld, J., Pozzer, A., Pöschl, U., Fnais, M., Haines, A., Münzel, T., 2020. Loss of life expectancy from air pollution compared to other risk factors: a worldwide perspective. Cardiovasc. Res. 116 (11), 1910–1917.
Levy, R.C., Remer, L.A., Mattoo, S., Vermote, E.F., Kaufman, Y.J., 2007. Second-generation operational algorithm: retrieval of aerosol properties over land from inversion of Moderate Resolution Imaging Spectroradiometer spectral reflectance. J. Geophys. Res. Atmos. 112 (D13).
Levy, R.C., Remer, L.A., Dubovik, O., 2007a. Global aerosol optical properties and application to Moderate Resolution Imaging Spectroradiometer aerosol retrieval over land. J. Geophys. Res. Atmos. 112 (D13).
Levy, R.C., Mattoo, S., Munchak, L.A., Remer, L.A., Sayer, A.M., Patadia, F., Hsu, N.C., 2013. The Collection 6 MODIS aerosol products over land and ocean. Atmos. Meas. Tech. 6 (11), 2989–3034.
Levy, R.C., Munchak, L.A., Mattoo, S., Patadia, F., Remer, L.A., Holz, R.E., 2015. Towards a long-term global aerosol optical depth record: applying a consistent aerosol retrieval algorithm to MODIS and VIIRS-observed reflectance. Atmos. Meas. Tech. 8 (10), 4083–4110.
Li, R., Ma, T., Xu, Q., Song, X., 2018. Using MAIAC AOD to verify the PM2. 5 spatial patterns of a land use regression model. Environ. Pollut. 243, 501–509.
Lin, C., Li, Y., Yuan, Z., Lau, A.K., Li, C., Fung, J.C., 2015. Using satellite remote sensing data to estimate the high-resolution distribution of ground-level PM2. 5. Rem. Sens. Environ. 156, 117–128.
Liu, Y., Sarnat, J.A., Kilaru, V., Jacob, D.J., Koutrakis, P., 2005. Estimating ground-level PM2. 5 in the eastern United States using satellite remote sensing. Environ. Sci. Technol. 39 (9), 3269–3278.
Liu, Y., Franklin, M., Kahn, R., Koutrakis, P., 2007. Using aerosol optical thickness to predict ground-level PM2. 5 concentrations in the St. Louis area: a comparison between MISR and MODIS. Rem. Sens. Environ. 107 (1–2), 33–44.
Lyapustin, A., Wang, Y., Xiong, X., Meister, G., Platnick, S., Levy, R., et al., 2014. Scientific impact of MODIS C5 calibration degradation and C6+ improvements. Atmos. Meas. Tech. 7 (12), 4353–4365.
Ma, Z., Hu, X., Huang, L., Bi, J., Liu, Y., 2014. Estimating ground-level PM2. 5 in China using satellite remote sensing. Environ. Sci. Technol. 48 (13), 7436–7444.
Mei, L., Strandgren, J., Rozanov, V., Vountas, M., Burrows, J.P., Wang, Y., 2019. A study of the impact of spatial resolution on the estimation of particle matter concentration from the aerosol optical depth retrieved from satellite observations. Int. J. Rem. Sens. 40 (18), 7084–7112.
Müller, I., Erbertseder, T., Taubenböck, H., 2022. Tropospheric NO2: explorative analyses of spatial variability and impact factors. Rem. Sens. Environ. 270, 112839.
Munchak, L.A., Levy, R.C., Mattoo, S., Remer, L.A., Holben, B.N., Schafer, J.S., et al., 2013. MODIS 3 km aerosol product: applications over land in an urban/suburban region. Atmos. Meas. Tech. 6 (7), 1747–1759.
North, P., Heckel, A., 2019. Algorithm theoretical basis document – annex C (SU-SLSTR). Copernicus climate change Service (C3S). http://datastore.copernicus-climate.eu/documents/satellite-aerosol-properties/C3S_D312b_Lot2.1.2.2_v1.1_201902_ATBD_AER_v1.1_and_annexes.zip.
Popp, T., the C3S_312b_Lot2 aerosol team, 2019. Product user guide and specification – aerosol products. Copernicus climate change Service (C3S). http://datastore.copernicus climate.eu/documents/satellite-aerosolproperties/C3S_D312b_Lot2.3.2.2_v1.1_201902_PUGS_AER_v1.1.pdf.
Putaud, J.P., Raes, F., Van Dingenen, R., Brüggemann, E., Facchini, M.C., Decesari, S., et al., 2004. A European aerosol phenomenology—2: chemical characteristics of particulate matter at kerbside, urban, rural and background sites in Europe. Atmos. Environ. 38 (16), 2579–2595.
Remer, L.A., Kaufman, Y.J., Tanré, D., Mattoo, S., Chu, D.A., Martins, J.V., et al., 2005. The MODIS aerosol algorithm, products, and validation. J. Atmos. Sci. 62 (4), 947–973.
Remer, L.A., Tanré, D., Kaufman, Y.J., Levy, R., Mattoo, S., 2006. Algorithm for Remote Sensing of Tropospheric Aerosol from MODIS: Collection 005. National Aeronautics and Space Administration, p. 1490.
Remer, L.A., Mattoo, S., Levy, R.C., Munchak, L.A., 2013. MODIS 3 km aerosol product: algorithm and global perspective. Atmos. Meas. Tech. 6 (7), 1829–1844.
Rubin, J.I., Collins, W.D., 2014. Global simulations of aerosol amount and size using MODIS observations assimilated with an Ensemble Kalman Filter. J. Geophys. Res. Atmos. 119 (22), 12–780.
Schaap, M., Apituley, A., Timmermans, R.M.A., Koelemeijer, R.B.A., Leeuw, G.D., 2009. Exploring the relation between aerosol optical depth and PM 2.5 at Cabauw, The Netherlands. Atmos. Chem. Phys. 9 (3), 909–925.
Seidel, D.J., Zhang, Y., Beljaars, A., Golaz, J.C., Jacobson, A.R., Medeiros, B., 2012. Climatology of the planetary boundary layer over the continental United States and Europe. J. Geophys. Res. Atmos. 117 (D17).
Sheridan, P.J., Ogren, J.A., 1999. Observations of the vertical and regional variability of aerosol optical properties over central and eastern North America. J. Geophys. Res. Atmos. 104 (D14), 16793–16805.
Shi, L., Zanobetti, A., Kloog, I., Coull, B.A., Koutrakis, P., Melly, S.J., Schwartz, J.D., 2016. Low-concentration PM2. 5 and mortality: estimating acute and chronic effects in a population-based study. Environ. Health Perspect. 124 (1), 46–52.
Song, W., Jia, H., Huang, J., Zhang, Y., 2014. A satellite-based geographically weighted regression model for regional PM2. 5 estimation over the Pearl River Delta region in China. Rem. Sens. Environ. 154, 1–7.
Sorek-Hamer, M., Kloog, I., Koutrakis, P., Strawa, A.W., Chatfield, R., Cohen, A., et al., 2015. Assessment of PM2. 5 concentrations over bright surfaces using MODIS satellite observations. Rem. Sens. Environ. 163, 180–185.
Sorek-Hamer, M., Just, A.C., Kloog, I., 2016. The use of satellite remote sensing in epidemiological studies. Curr. Opin. Pediatr. 28 (2), 228.
Stachelek, J., 2014. Interpolation via Inverse Path Distance Weighting.
Sun, K., Zhu, L., Cady-Pereira, K., Chan Miller, C., Chance, K., Clarisse, L., et al., 2018. A physics-based approach to oversample multi-satellite, multispecies observations to a common grid. Atmos. Meas. Tech. 11 (12), 6679–6701.
Tian, J., Chen, D., 2010. A semi-empirical model for predicting hourly ground-level fine particulate matter (PM2. 5) concentration in southern Ontario from satellite remote sensing and ground-based meteorological measurements. Rem. Sens. Environ. 114 (2), 221–229.
Toth, T.D., Zhang, J., Campbell, J.R., Hyer, E.J., Reid, J.S., Shi, Y., Westphal, D.L., 2014. Impact of data quality and surface-to-column representativeness on the PM 2.5/satellite AOD relationship for the contiguous United States. Atmos. Chem. Phys. 14 (12), 6049–6062.
Van de Kassteele, J., Koelemeijer, R.B.A., Dekkers, A.L.M., Schaap, M., Homan, C.D., Stein, A., 2006. Statistical mapping of PM10 concentrations over Western Europe using secondary information from dispersion modeling and MODIS satellite observations. Stoch. Environ. Res. Risk Assess. 21 (2), 183–194.
Van Donkelaar, A., Martin, R.V., Brauer, M., Kahn, R., Levy, R., Verduzco, C., Villeneuve, P.J., 2010. Global estimates of ambient fine particulate matter concentrations from satellite-based aerosol optical depth: development and application. Environ. Health Perspect. 118 (6), 847–855.

Van Donkelaar, A., Martin, R.V., Brauer, M., Boys, B.L., 2015. Use of satellite observations for long-term exposure assessment of global concentrations of fine particulate matter. Environ. Health Perspect. 123 (2), 135–143.
Veefkind, J.P., Van der Hage, J.C.H., Ten Brink, H.M., 1996. Nephelometer derived and directly measured aerosol optical depth of the atmospheric boundary layer. Atmos. Res. 41 (3–4), 217–228.
Veefkind, J.P., de Leeuw, G., Durkee, P.A., 1998. Retrieval of aerosol optical depth over land using two-angle view satellite radiometry during TARFOX. Geophys. Res. Lett. 25 (16), 3135–3138.
Viatte, C., Clerbaux, C., Maes, C., Daniel, P., Garello, R., Safieddine, S., Ardhuin, F., 2020. Air pollution and sea pollution seen from space. Surv. Geophys. 41 (6), 1583–1609.
Wang, B., Chen, Z., 2016. High-resolution satellite-based analysis of ground-level PM2. 5 for the city of Montreal. Sci. Total Environ. 541, 1059–1069.
World Health Organization, 2021. WHO Global Air Quality Guidelines: Particulate Matter (PM2. 5 and PM10), Ozone, Nitrogen Dioxide, Sulfur Dioxide and Carbon Monoxide.
Wu, J., Liang, J., Zhou, L., Yao, F., Peng, J., 2019. Impacts of AOD correction and spatial scale on the correlation between high-resolution AOD from gaofen-1 satellite and in situ PM2. 5 measurements in shenzhen city, China. Rem. Sens. 11 (19), 2223.
Xie, Y., Wang, Y., Zhang, K., Dong, W., Lv, B., Bai, Y., 2015. Daily estimation of ground-level PM2. 5 concentrations over Beijing using 3 km resolution MODIS AOD. Environ. Sci. Technol. 49 (20), 12280–12288.
Xu, J.W., Martin, R.V., Van Donkelaar, A., Kim, J., Choi, M., Zhang, Q., et al., 2015. Estimating ground-level PM 2.5 in eastern China using aerosol optical depth determined from the GOCI satellite instrument. Atmos. Chem. Phys. 15 (22), 13133–13144.
Yao, F., Palmer, P.I., 2021. A model framework to reduce bias in ground-level PM2. 5 concentrations inferred from satellite-retrieved AOD. Atmos. Environ. 248, 118217.
Yao, F., Si, M., Li, W., Wu, J., 2018. A multidimensional comparison between MODIS and VIIRS AOD in estimating ground-level PM2. 5 concentrations over a heavily polluted region in China. Sci. Total Environ. 618, 819–828.
You, W., Zang, Z., Pan, X., Zhang, L., Chen, D., 2015. Estimating PM2. 5 in Xi'an, China using aerosol optical depth: a comparison between the MODIS and MISR retrieval models. Sci. Total Environ. 505, 1156–1165.
Zhang, Y., Li, Z., 2015. Remote sensing of atmospheric fine particulate matter (PM2. 5) mass concentration near the ground from satellite observation. Rem. Sens. Environ. 160, 252–262.
Zhang, H., Hoff, R.M., Engel-Cox, J.A., 2009. The relation between Moderate Resolution Imaging Spectroradiometer (MODIS) aerosol optical depth and PM2. 5 over the United States: a geographical comparison by US Environmental Protection Agency regions. J. Air Waste Manag. Assoc. 59 (11), 1358–1369.
Zhang, Y., Li, Z., Bai, K., Wei, Y., Xie, Y., Zhang, Y., et al., 2021. Satellite remote sensing of atmospheric particulate matter mass concentration: advances, challenges, and perspectives. Fundamen. Res. 1 (3), 240–258.
Zheng, Y., Zhang, Q., Liu, Y., Geng, G., He, K., 2016. Estimating ground-level PM2. 5 concentrations over three megalopolises in China using satellite-derived aerosol optical depth measurements. Atmos. Environ. 124, 232–242.
Zou, B., Pu, Q., Bilal, M., Weng, Q., Zhai, L., Nichol, J.E., 2016. High-resolution satellite mapping of fine particulates based on geographically weighted regression. Geosci. Rem. Sens. Lett. IEEE 13 (4), 495-49.